Article:

Microstructural Evolution of Copper-Titanium Alloy during In-situ Formation of TiB$_2$ Particles

M.Sobhani[† 1], H.Arabi[1], A.Mirhabibi[2]

[1]Center of Excellence for Advanced Materials and Processing, (CEAMP) School of Metallurgy and Materials Engineering, Iran University of Science and Technology, IUST, Tehran, Iran

[2]Center of Excellence for Ceramic Materials in Energy and Environmental Applications (CECMEEA), IUST, Tehran, 16845-118, Iran

Abstract

Bulk Cu-Ti alloy reinforced by TiB$_2$ nano particles was prepared using in-situ reaction between Cu-3.4wt.% Ti and Cu-0.7wt.% B along with rapid solidification and subsequent heat treatment for 1-10 hrs at 900ºC. High-resolution transmission electron microscopy (HRTEM) characterization showed that primary TiB$_2$ nano particles and TiB whiskers were formed by in-situ reaction between Ti and B in the liquid copper. Formation of TiB whiskers within the melt led to coarsening of TiB$_2$ particles. Primary TiB$_2$ particles were dispersed along the grain boundaries and hindered grain growth at high temperature while the secondary TiB$_2$ particles were formed during heat treatment of the alloy by diffusion reaction of solute titanium and boron inside the grains. Electrical conductivity and hardness of composite were evaluated during heat treatment. The results indicated that formation of secondary TiB$_2$ particles in the matrix caused a delay in hardness reduction at high temperature. The electrical conductivity increased along with hardness up to 8 hrs of heat treatment and reached 33.5% IACS and 158 HV, respectively.

Key words: In-situ reaction, TiB whiskers, TiB$_2$, Composite, Cu-Ti

1.Introduction

Copper and copper based alloys are widely used in numerous applications that require high mechanical properties along with high electrical and thermal conductivity. Mechanical strength of copper can be increased by age hardening or incorporating non-metallic second phase particles such as oxides and boride in its matrix. Adding elements such as Be, Cr, Zr and Ti to copper melt, which have low solvability in

---

[†] Corresponding Author , P.O. Box 16845-118, Tehran Iran, FAX: (+9821)77240480 , TEL: (+9821) 77459151, E-mail: m_sobhani@iust.ac.ir

copper at lower temperatures, can lead to precipitation of hard secondary phases by age hardening. These precipitates are frequently grown during ageing or working at high temperature, which leads to decrease in electrical conductivity and mechanical properties of alloys. Cu–Ti alloys that are susceptible to age hardening can be a possible substitute for the expensive and toxic age hardened Cu–Be alloys since they have good thermal stability and high temperature strength [1-3]. However, Ti as a partial solute element can reduce electrical conductivity of copper in case that more than 1 wt.% of this element is added to its chemical content [4]. It has been reported that, by increasing Ti content, electrical conductivity of copper matrix decreases dramatically as negative effect of Ti on electrical properties of copper alloys is more than that of other common alloying elements such as Zn, Sn and Ni. On the other hand, a low amount of Ti does not lead to precipitation of the required phases for strengthening Cu -Ti alloys [5]. Hence, low mechanical properties of this type of alloys are obtained. In order to compensate for the effects of low amount of Ti in copper, TiB_2 particles may be used for reinforcement. TiB_2 nano particles can be formed in molten copper by an in-situ reaction between boron and titanium [6]. TiB_2 addition to copper alloys greatly increases their stiffness, hardness and wear-resistance and decreases coefficients of thermal expansion (CTE) of this type of alloys [7]. Moreover, harmful effect of the dispersed TiB_2 particles on electrical conductivity of copper is much less than that of other ceramic reinforced particles [8,9]. Previous researches [10] have shown that TiB_2 particles can act as a grain growth inhibitor at high temperature; thereby, these particles can preserve high temperature mechanical strength of copper alloy. Moreover, these particles can have a positive effect on precipitating behavior of Cu-Ti alloys [11].

Manufacturing technology of metal matrix composites through cast process is of particular interest due to its lower cost and potential for mass production. Although there are some reports on the effect of TiB_2 particles on copper matrix strengthening via various methods such as powder metallurgy [12], melt mixing [13] and mechanical alloying [8], no reports have been published yet about the mechanism of in-situ formation of TiB_2 particles in Cu-Ti alloy prepared by cast method. In the current work, Cu-Ti-TiB_2 composite was produced via a cast process. The purpose of this work was to study evolution of in-situ formation of TiB_2 particles in rapid solidified Cu-Ti-TiB_2 as well as hardness and electrical properties of the produced composite.

2. Experimental Method

In order to prepare Cu-1wt.%Ti-1wt.%TiB$_2$ in-situ composite, Cu-3.4wt.%Ti and Cu-0.7wt.%B master alloys were prepared from high-purity copper (OFHC), titanium plate (i.e. 99.99%) and boron powder (i.e.99.98%). The master alloys were separately melted in an alumina crucible via high vacuum (3.5 $\times10^{-2}$ mbar) induction melting furnace (VIM) and poured in a 50×50×100 mm^3 copper mold. Then, they were degreased in NaOH solution and cleaned in nitric acid 10%. In order to increase their melting rate and mix them simultaneously while avoiding gravity segregation of TiB$_2$ particles in the melt, the surface of two master alloys was coupled and charged in the VIM furnace. Coupled master alloy was melted in a vacuum induction furnace at 1200°C and, just after melting, the melt mixture was poured in the water-cooled copper die. Heat treatment of cast ingots was performed in the molten salt bath with equal weight percent of NaCl and CaCO$_3$ at 900°C for 1 to 10 hrs. Thin slices were cut from the heat treated samples using ISOMET low speed cutting machine and polished mechanically up to 15μm. 3mm diameter disks were punched out from these samples and then they were electro-polished via a jet electropolisher using solution of 35 % nitric acid and 65% methanol at -30ºC at voltage of 12V. Various samples of as-cast and heat treated composite were investigated by high-resolution transmission electron microscopy (HRTEM) equipped with electron energy loss spectroscopy (EELS) and field emission gun scanning electron microscope (FEG-SEM). Micro hardness tests were performed using Vickers hardness tester under 50 g load. Electrical conductivity in % IACS (International Annealed Copper Standard) of the samples was measured using four-point probe method at room temperature according to ASTM B-193 standard. In order to compare effect of TiB$_2$ on microstructure and electrical properties of the composite, a reference sample with Cu-3.4 wt.% Ti composition was prepared in the same condition as Cu-Ti-TiB$_2$ composite. All the tests performed in the composite were also performed on this reference sample.

3. Results and Discussion

In order to determine the reaction direction and synthesis products in the Cu-Ti-B system, the Gibbs free energy of feasible chemical reactions in molten copper was calculated according to thermodynamic data from [14] and the results are shown in Fig. 1. Thermodynamic calculation showed that all feasible reactions

had a negative change in Gibbs free energy. Nevertheless, due to the lowest free energy of TiB_2 among the five possible products, formation of TiB_2 in molten copper was more susceptible than that of other components.

Thermodynamically stable TiB_2 particles can be formed due to a chemical reaction between elemental boron and titanium at titanium melt micelle interface in molten copper according to Gou et al.'s model [15]. Since the melting point of Cu-Ti and Cu-B master alloys was close to each other, they were simultaneously begun to melt and mix in the crucible. The diffusion rate of boron element should be higher than that of Ti element due to higher fluidity of Cu-B alloy melt than that of Cu-Ti at the same temperature. Thus, it can be concluded that boron element could be diffused through Cu-Ti melt micelles interface. At this moment, there is much greater interface between Cu-B and Cu-Ti melt micelles could lead to formation of many nano TiB_2 particles. Moreover, with the formation of TiB_2 particles and consumption of Ti, the molar ratio of Ti/B is possible to reach 1 at micelle interface. Therefore, in this condition, diffusion of boron through Cu-Ti melt micelle interface also could lead to formation of TiB particles.

BS-SEM micrograph of rapid solidified sample obtained from C-Ti-B alloy melt is shown in Fig. 2. As can be seen in this figure, two types of morphology of the reinforced particles were determined within the matrix. The needlelike dark particles (Fig.2.a) were identified as TiB whiskers by TEM and selected area diffraction (SAD) pattern, as shown in Fig .3. It is likely that TiB whiskers were formed in Cu-Ti-B melt by chemical reaction between Ti and B in molten copper due to boron diffusion through the melt micelle interface, as mentioned previously. The second type particles which also had an irregular shape and were especially dispersed along the grain boundaries were identified as TiB_2 particles (see Fig. 2.b).

As seen in Fig. 2.a, TiB_2 particles, which were connected to TiB whiskers, had larger size than the separated ones. From this evidence, it can be concluded that the formation of TiB whisker can be resulted in coarsening TiB_2 particles. Increase in the particle size of TiB_2 particles by formation of TiB whiskers can be analyzed by considering the amount of latent heat released due to the formation of TiB whiskers and TiB_2 particles in the melt. The formation of TiB_2 particles as well as TiB whiskers in the molten copper caused to release latent heat of formation of each particle (i.e. TiB, TiB_2) in the melt and led to increased temperature at reaction interface. The amount of released heat and rising temperature depended on micelle size and mass balance at reaction interface [15, 16]. Thermodynamic calculation showed that latent heat

4

release due to in-situ formation of one mole TiB_2 at 1200 °C could increase one mole of copper temperature from 1200 °C up to about 8000 °C. This temperature was enough for melting and/or welding TiB_2 particles during in-situ reaction. In other words, according to Ti-B phase diagram [17], this temperature was high enough to form the new TiB_2 particles at congruent temperature (i.e.3225 ºC) and led to coarsening TiB_2 particles in molten copper.

The temperature risen at reaction interface also could result in gas generation due to copper evaporation. Fig. 4 shows the microstructure of as-cast composite with dot point map of elements. As demonstrated in this figure, the arrangement of TiB_2 particles was in the form of burst bubble that can be seen in the region with high concentration of TiB_2 particles, which clearly confirmed the gas generation due to formation of TiB_2 particles which could be only observed in the area with a large amount of released heat. This is in agreement with the reported work of Dallaire et al. [18] who stated that the formation of TiB_2 particles could lead to copper evaporation.

Microstructure of composite after 10 hrs of heat treatment is shown in Fig. 5.a. As shown in this figure, a part of TiB_2 particles was dispersed along the grain boundaries. The distribution of TiB_2 particles as well as particle size was affected by many factors including in-situ reaction condition and element concentration [15, 16]. The density and wetting angle are also two effective factors on distribution of TiB_2 particles. Because of differences between Cu and TiB_2 densities, i.e. 8.9 g/cm^3 and 4.95 g/cm^3 respectively, and low wettability of TiB_2 particles by molten copper (i.e. wetting angle=136 º) [19], a larger size of TiB_2 particles was repulsed and redistributed toward the melt freezing interface and finally to grain boundaries while the majority of nano sized particles was remained inside the grain according to solid/liquid interface theories for MMCs [20,21]. From Fig. 5.a, it can be seen that TiB_2 particles were pinned the grain boundaries and caused significant decrease in grain size of the composite. This decrease in grain size with the presence of TiB_2 particles clearly indicated that TiB_2 particles could act as grain refinement in α-Cu. This is in accordance with other researchers [7] who also reported that the presence of TiB_2 particles in grain boundaries could lead to reduction in grain size and hinder grain growth at high temperature. Fig. 5.b shows the distribution of TiB whiskers along the grain boundary after deep etching at HNO_3, which clearly shows that TiB whiskers along with coarse TiB_2 particles also were redistributed by melt freezing interface to grain boundaries.

5

Effect of heat treatment on microstructure of composite was evaluated by TEM. Fig. 6. shows TEM image of composite with jump ratio map of elements via EELS after 6 hrs of heat treatment at 900 ºC. As seen in this figure, the aggregation of Ti was not completely in alignment with B atoms. This distribution of elements within the matrix indicated that rapid solidification could suppress chemical reaction between boron and titanium atoms and consequently formation of TiB_2 particles in molten copper. In other words, as in-situ formation of TiB_2 particles in molten copper was a time-consuming reaction, due to being controlled by diffusion of boron through melt micelles interfaces, a part of boron might be left within the matrix after rapid solidification. During heat treatment of composite at 900 ºC, boron and titanium atoms can react with each other. The result of this reaction was formation of Ti/B compound at the diffusion reaction interface, as shown with arrow A in Fig. 6.a. Corresponding to TEM image with SAD pattern and chemical analysis results in Fig. 6, it was identified that Ti/B compound consistent with stoichiometry composition of TiB_2 particles as their crystal structure was hexagonal with lattice parameter of a=0.303 nm and c=0.323 nm.

The effect of further heat treatment on formation of TiB_2 particles is shown in Fig. 7. As shown in this figure, the formation of secondary TiB_2 was associated with refining TiB_2 particles by being driven out of the remained copper from TiB_2 structure, as indicated by refining zone in Fig. 7.a. The final structure of this reaction was TiB_2 particles with hexagonal structure, which was confirmed by FFT pattern in Fig. 7.b.

Effect of heat treatment on hardness and grain size of composite in comparison to Cu-3.4 wt.% Ti alloy is shown in Fig. 8. The hardness of composite gradually increased as time of heat treatment increased. The maximum hardness of composite (i.e. 158 HV) was achieved after 8 hrs of heat treatment. This increase in hardness value apparently up to 8 hrs of heat treatment was most likely due to formation of secondary TiB_2 particles, as mentioned previously. Based on this result, it could be reasoned that reinforced particles can act as a barrier to the movement of dislocation in composite. Thus, more reinforcement particles in the matrix might correspondingly brought greater increase in hardness. After 8 hrs of heat treatment, decrease of hardness happened and effect of secondary TiB_2 formation was completely revoked. Nevertheless, decrease in hardness after peak value was not remarkable and was attributed to pinning effects of TiB_2 particles at grain boundaries, which hindered grain growth at high temperature. Fig. 8.b shows variation of grain size of composite and binary Cu-3.4 wt.% Ti alloy versus heat treatment time. The as-cast composite

6

had mean grain size of about 35μm and gradually increased up 10 hrs of heat treatment while the mean grain size of binary Cu-3.4 wt.% Ti sharply increased from 200 μm to about 1 mm after 10 hrs of heat treatment. The grain growth of binary Cu-Ti followed a relationship of the form of $D=Kt^n$, in which the constant parameters were determined as n=0.51 and k=35.69. This issue indicated that the velocity of grain boundary migration was not a linear function of driving force (i.e. delta G) while the rate of grain growth of composite was found to be constant during a period of 10 hrs of heat treatment. By comparing Fig. 8.a and Fig.8.b, it can be concluded that formation of primary TiB_2 particles, which dispersed at grain boundaries, reduced grain size and hindered grain growth while formation of secondary TiB_2 particles, which were formed during heat treatment inside the grain, postponed reduction in hardness during high temperature heat treatment.

Electrical conductivity of the composite was evaluated during heat treatment and results of this study indicated that electrical conductivity of as-cast composite was 15 % IACS and increased up to 33.5 % IACS after 8 hrs of heat treatment and saturated to about 34 % IACS after 10 hrs of heat treatment. As titanium significantly reduced electrical conductivity of copper [4], formation of secondary TiB_2 particles within the matrix consume dissolved titanium in the matrix and resulted in increased electrical conductivity. In other words, increase in resistivity due to the increasing volume fraction of TiB_2 particles was less than the amount of decrease in resistivity due to removal of Ti from the matrix; thereby, resulting in an overall increase in electrical conductivity of composite during heat treatment. This increase in electrical conductivity was mainly due to reduction of scattering surface of conductive electrons according to Nordheim rule [4]. As shown in Fig. 8.b, the grain size of composite was almost constant during heat treatment; thus, it can be concluded that hardness of composite was almost independent from grain size and mainly affected by formation of secondary TiB_2 particles. This finding along with the fact that electrical conductivity of composite increased during heat treatment exhibited that rapid solidified composite can be used for electrical application such as spot welding electrodes, that require high hardness stability at high temperature along with high electrical conductivity.

4. Conclusions

1- Cu-Ti-TiB$_2$ in-situ composite was successfully produced by the reaction of Cu-Ti and Cu-B master alloys.

2- In-situ reaction in Cu-Ti-B system caused the formation of TiB whiskers and TiB$_2$ particles in the matrix.

3- The formation of TiB whiskers resulted in coarsening of TiB$_2$ particles.

4- Primary TiB$_2$ particles formed in molten copper were dispersed along the grain boundaries and acted as an effective grain growth inhibitor. The secondary TiB$_2$ particles were formed in solid-state condition; these particles were formed inside the grains and increased hardness and electrical conductivity of composite during heat treatment.

5- Maximum value of hardness and electrical conductivity of composite were obtained after 8 hrs of heat treatment at 900º C which were 33.5 %IACS and 158 HV, respectively.

References

[1] Tu J. P, Rong W, Guo S Y, Yang Y Z. Dry sliding wear behavior of in situ Cu–TiB$_2$ nano-composites against medium carbon steel [J]. Wear, 2003, 255: 832-835.

[2] Tjong S C, Lau K C. Abrasive wear behavior of TiB$_2$ particle-reinforced copper matrix composites [J].Material Science and Engineer A, 2000, 282: 183-186.

[3] Soffa W A, Laughlin D E. High-strength age hardening copper–titanium alloys: redivivus [J]. Progress in Material Science.2004, 49: 347-366.

[4] Nagarjuna S, Balasubramanian K, Sarma D S. Effect of Ti additions on the electrical resistivity of copper [J]. Material Science and Engineer A, 1997, 225 :118-124.

[5] Nagarjuna S, Srinivas M, Balasubramanian K, Sarma D S. On the variation of mechanical properties with solute content in Cu- Ti alloys [J]. Material Science and Engineer A, 1999, 259:34-42.

[6] Tu J P, Wang N Y, Yang Y Z, Qi W X, Liu F, Zhang X B. Preparation and properties of TiB$_2$ nanoparticle reinforced copper matrix composites by in situ processing [J]. Materials Letters, 2002, 52: 448-452.

[7] Ma Z Y, Tjong S C. High temperature creep behavior of in-situ TiB$_2$ particulate reinforced copper-based composite [J]. Material Science and Engineer A, 2000, 284: 70-76.

[8] Dong S J, Zhou Y, Shi Y W, Chang B H. Formation of a TiB$_2$ Reinforced Copper-Based Composite by Mechanical Alloying and Hot Pressing[J]. Metallurgical and Materials Transaction A, 2002, 33: 1-6.

[9] Yid P, Chung D D L. Titanium diboride copper matrix composite [J]. Journal of material Science, 1997, 32: 1703-1709.

[10] Biselli C, Morris D G, Randall N. Mechanical alloying of high-strength copper alloys containing TiB$_2$ and Al$_2$O$_3$ dispersed particles [J]. Scripta Materials, 1994, 30(10):1327-1332.

[11] Bozic D, Stasic J, Ruzic J, Vilotijevic M, Rajkovic V, Synthesis and properties of a Cu-Ti-TiB$_2$ composite hardened by multiple Mechanisms[J]. Material Science and Engineer A, 2011, 528: 8139-8144.

9

[12] Kwon Y S. Microstructure changes in TiB_2-Cu nano composite under sintering [J]. Journal of Martial Science, 2004, 39: 5325-5331.

[13] Kim J H, Yun J H, Park Y H, Choa K M, Choi I D, Park I M, Manufacturing of Cu-TiB_2 composites by turbulent in situ mixing process [J]. Material Science and Engineer A, 2007, 449-451 :1018–1021.

[14] Binnewies M, Milke E. Thermochemical data of elements and compounds [M]. Wienheim, Wiley-VCH, 2002.

[15] Guo M, Shen K, Wang M. Relationship between microstructure, properties and reaction conditions for Cu-TiB_2 alloys prepared by in situ reaction [J]. Acta Materialia, 2009, 57:4568-4579.

[16] Guo M X, Wang M P, K Shen, Cao L F, Li Z, Zhang Z. Synthesis of nano TiB_2 particles in copper matrix by in situ reaction of double-beam melt[J]. Journal of Alloys and Compounds,2008,460:585-589.

[17] Xiaoyan Ma, Changrong Li, Zhenmin Du, Weijing Zhang. Thermodynamic assessment of the Ti-B system [J]. Journal of alloys and compounds, 2004, 370:149-158.

[18] Dallaire S, Legoux J. Synthesis of TiB_2 in liquid copper [J]. Material Science and Engineer A, 1994, 183:139-144.

[19] Yasinskaya G A. The wetting of refractory carbides, borides, and nitrides by molten metals [J]. Soviet Powder Metallurgy and Metal Ceramics, 1966, 5/7: 557-559.

[20] Shangguan D, Ahuja S, Stefanescu D M. An Analytical Model for the Interaction between an Insoluble Particle and an Advancing Solid Liquid Interface [J]. Metallurgical Transaction A, 1992, 23: 669-680.

[21] Stefanescu D M, Dhindaw B K, Kacar S A, Moitra A. Behavior of Ceramic Particles at the Solid-Liquid Metal Interface in Metal Matrix Composites [J]. Metallurgical Transaction A, 1988, 19:2847-2855.
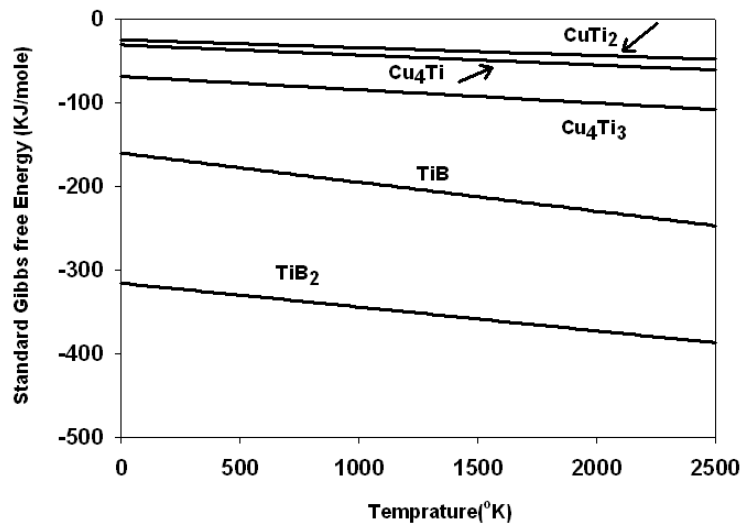
Figures caption

Fig.1. Variation of standard Gibbs free energy of feasible chemical reactions versus temperature in Cu-Ti-B system
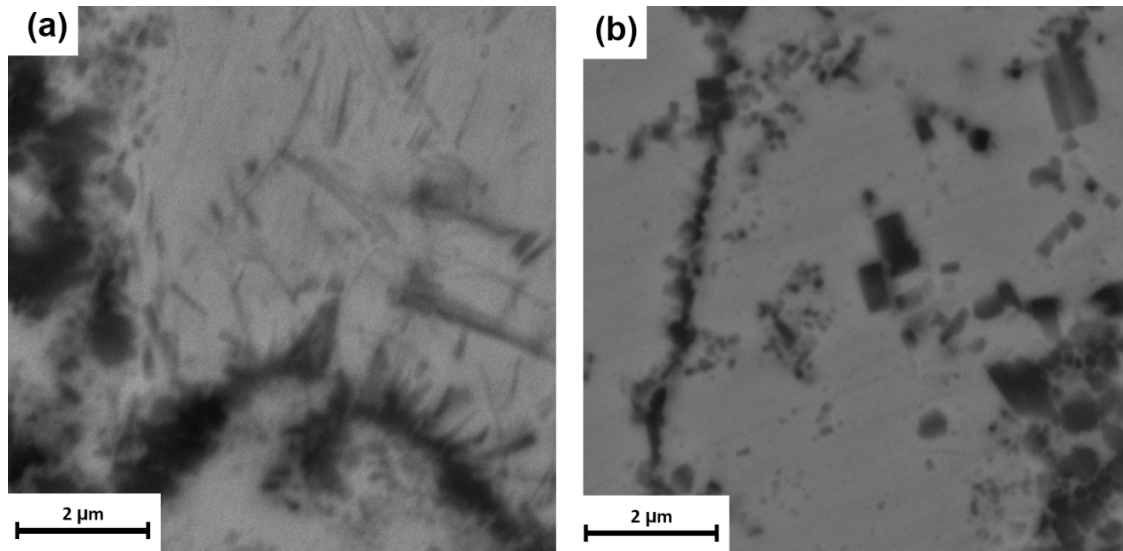
Fig.2. BS-SEM of as solidified composite shows (a) coarsening of TiB_2 particles due to formation of TiB whiskers (b) TiB_2 particles along the grain boundary
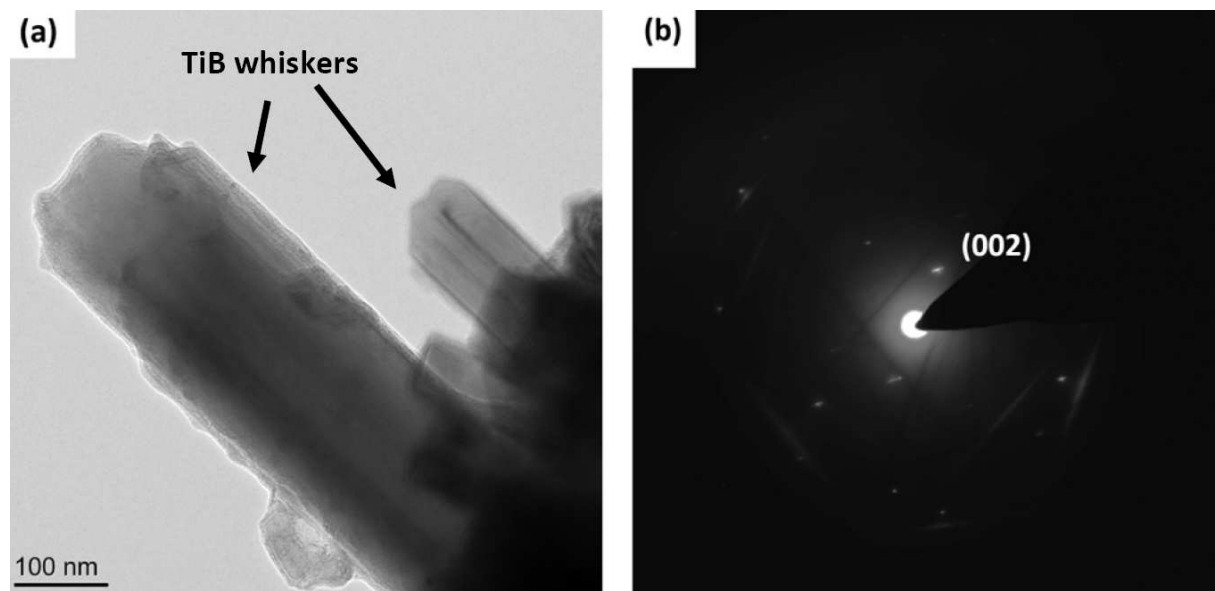
Fig.3. (a) TEM micrograph of TiB whiskers welded with TiB_2 particles (b) Kikuchi pattern of TiB whiskers
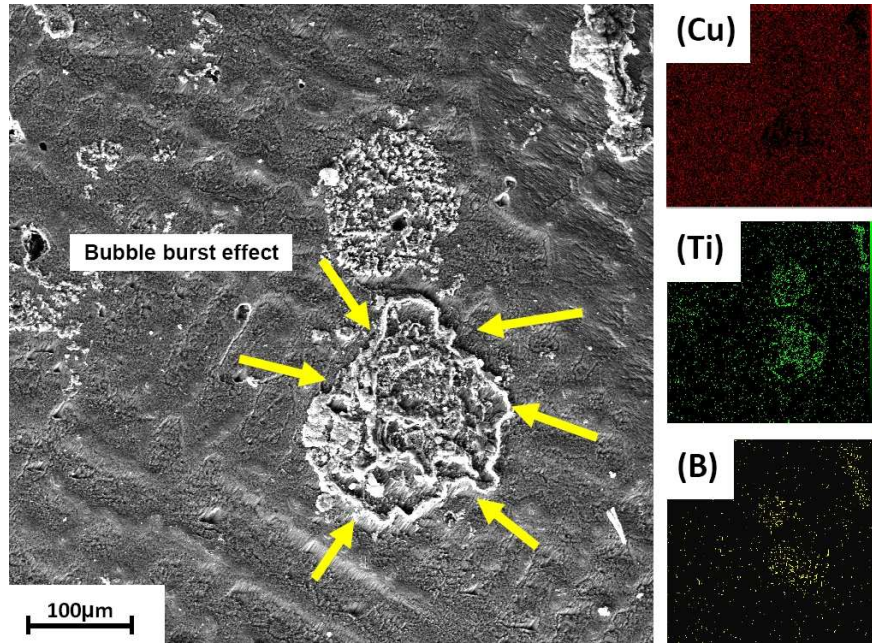
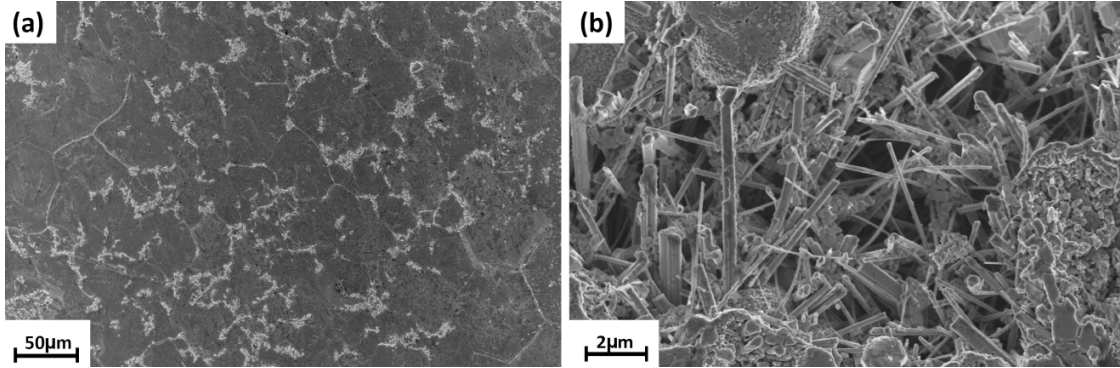Fig.4. As-cast micrograph of Cu-Ti-TiB_2 with map of Cu, Ti, B elements

Fig.5. (a) Distribution of TiB_2 particles in grain boundaries (b) TiB whiskers along with TiB_2 particles in grain boundary after deep etching in HNO_3

Fig.6. (a) TEM micrograph shows evolution in formation of secondary TiB_2 particles after 6 hrs of heat treatment with jump ratio elemental map (b) SAD pattern of TiB_2 particles

Fig.7. (a) HRTEM image of formation of secondary TiB_2 after 8 hrs of heat treatment at 900 ºC (b) FFT pattern of TiB_2

Fig.8. (a) Variation of harness and (b) grain size as a function of heat treatment time for Cu-Ti-TiB_2 composite and Cu-3.4wt.%Ti alloy

Fig.1. Variation of standard Gibbs free energy of feasible chemical reactions versus temperature in

Cu-Ti-B system

12

Fig.2. BS-SEM of as solidified composite shows (a) coarsening of TiB$_2$ particles due to formation of TiB whiskers (b) TiB$_2$ particles along the grain boundary

Fig.3. (a) TEM micrograph of TiB whiskers welded with TiB$_2$ particles (b) Kikuchi pattern of TiB whiskers

Fig.4. As-cast micrograph of Cu-Ti-TiB₂ with map of Cu, Ti, B elements

Fig.5. (a) Distribution of TiB$_2$ particles in grain boundaries (b) TiB whiskers along with TiB$_2$ particles in grain boundary after deep etching in HNO$_3$
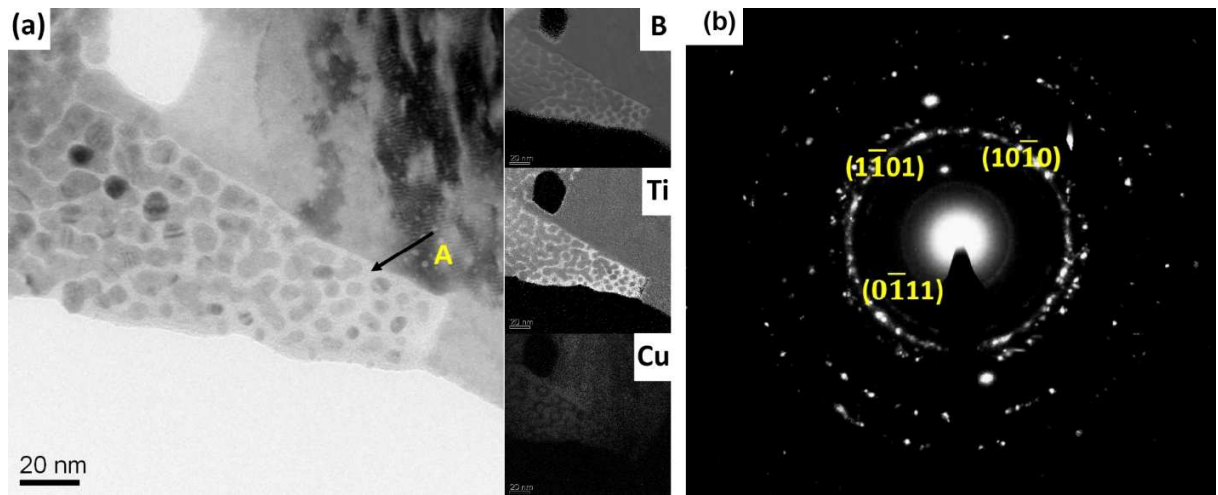
Fig.6. (a) TEM micrograph shows evolution in formation of secondary TiB₂ particles after 6 hrs of heat treatment with jump ratio elemental map (b) SAD pattern of TiB₂ particles
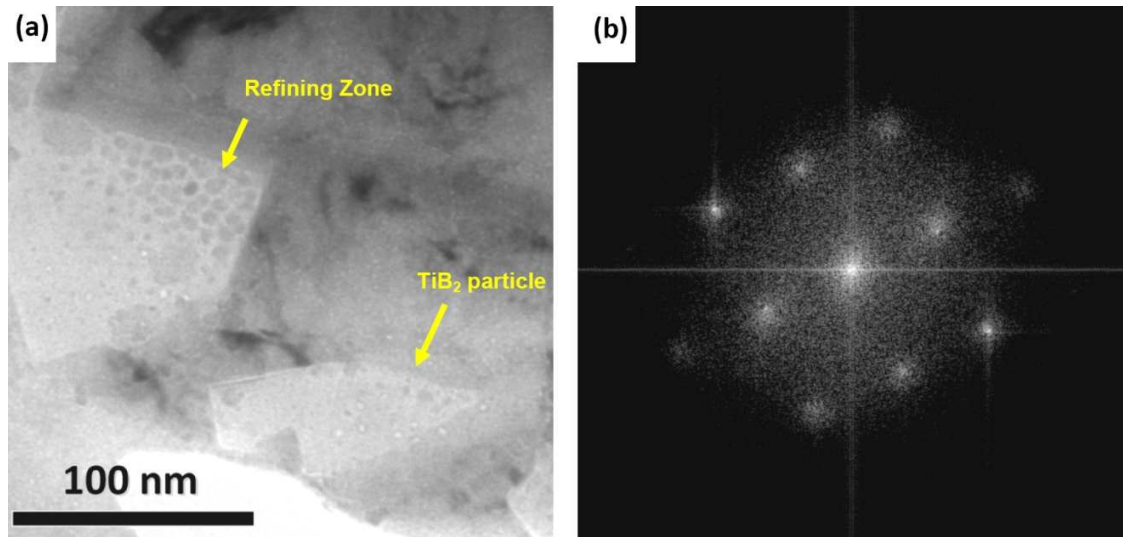
Fig.7. (a) HRTEM image of formation of secondary TiB$_2$ after 8 hrs of heat treatment at 900 ºC (b)
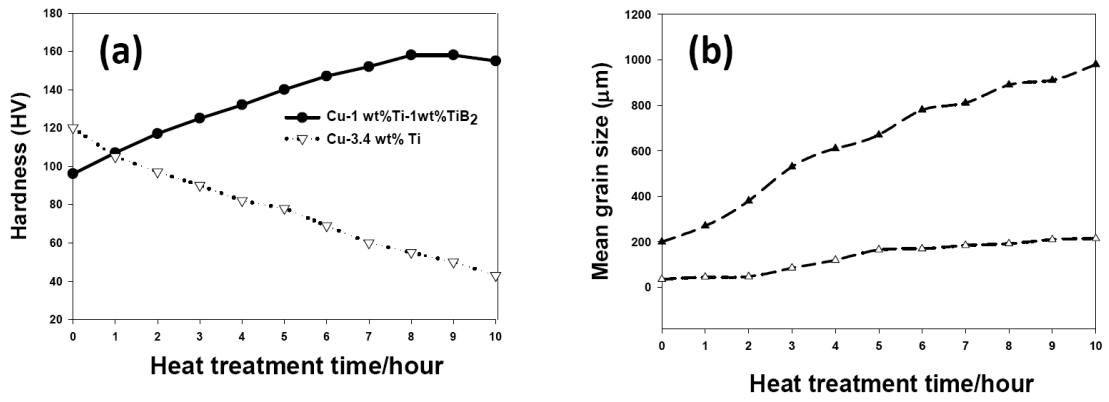
FFT pattern of TiB$_2$

Fig.8. (a) Variation of harness and (b) grain size as a function of heat treatment time for Cu-Ti-TiB$_2$ composite and Cu-3.4wt.%Ti alloy